

TOPICAL REVIEW

The preparation of magnetic nanoparticles for applications in biomedicine

Pedro Tartaj¹, María del Puerto Morales¹,
Sabino Veintemillas-Verdaguer, Teresita González-Carreño and
Carlos J Serna

Instituto de Ciencia de Materiales de Madrid, CSIC, Cantoblanco, 28049, Madrid, Spain

E-mail: ptartaj@icmm.csic.es and puerto@icmm.csic.es

Received 17 March 2003

Published 18 June 2003

Online at stacks.iop.org/JPhysD/36/R182

Abstract

This review is focused on describing state-of-the-art synthetic routes for the preparation of magnetic nanoparticles useful for biomedical applications. In addition to this topic, we have also described in some detail some of the possible applications of magnetic nanoparticles in the field of biomedicine with special emphasis on showing the benefits of using nanoparticles. Finally, we have addressed some relevant findings on the importance of having well-defined synthetic routes to produce materials not only with similar physical features but also with similar crystallochemical characteristics.

1. Introduction

Nanotechnology is beginning to allow scientists, engineers, and physicians to work at the cellular and molecular levels to produce major advances in the life sciences and healthcare. Real applications of nanostructured materials in life sciences are uncommon at the present time. However, the excellent properties of these materials when compared with their bulk counterparts provide a very promising future for their use in this field [1–3].

Nanoclusters are ultrafine particles of nanometre dimensions located in the transition region between molecules and microscopic (micron-size) structures. Viewed as molecules, they are so large that they provide access to realms of quantum behaviour that are not otherwise accessible; viewed as materials, they are so small that they exhibit characteristics that are not observed in larger (even 100 nm) structures. It is in this size regime that many recent advances have been made in biology, physics, and chemistry [4]. For example, when the particle dimensions of semiconductor materials become comparable to, or smaller than the Bohr radius, an increase in the energy band gap is observed [5–8]. In noble metals,

the decrease in size below the electron mean free path (the distance the electron travels between scattering collisions with the lattice centres) gives rise to intense absorption in the visible–near-UV region [9]. Metal nanoparticles also exhibit a broad range of fascinating mechanical behaviour such as superplasticity [10]. Ceramic materials composed of powders with a particle size in the nanometric range are also receiving attention because they may significantly enhance sintering rates or dramatically lower sintering temperatures [11–14]. Also, ceramic matrix composites with dispersed nanoparticles have better mechanical properties [10, 15].

Magnetic nanoparticles show remarkable new phenomena such as superparamagnetism, high field irreversibility, high saturation field, extra anisotropy contributions or shifted loops after field cooling. These phenomena arise from finite size and surface effects that dominate the magnetic behaviour of individual nanoparticles [16]. Frenkel and Dorfman [17] were the first to predict that a particle of ferromagnetic material, below a critical particle size (< 15 nm for the common materials), would consist of a single magnetic domain, i.e. a particle that is a state of uniform magnetization at any field. The magnetization behaviour of these particles above a certain temperature, i.e. the blocking temperature, is identical to that of atomic paramagnets (superparamagnetism) except that an

¹ Authors to whom correspondence should be addressed.

extremely large moment and thus, large susceptibilities are involved [18].

Industrial applications of magnetic nanoparticles cover a broad spectrum such as magnetic seals in motors, magnetic inks for bank cheques, magnetic recording media and biomedical applications such as magnetic resonance contrast media and therapeutic agents in cancer treatment [19–22]. Each potential application requires the magnetic nanoparticles to have different properties. For example, in data storage applications, the particles need to have a stable, switchable magnetic state to represent bits of information, a state that is not affected by temperature fluctuations.

For biomedical applications the use of particles that present superparamagnetic behaviour at room temperature (no remanence along with a rapidly changing magnetic state) is preferred [23–25]. Furthermore, applications in biology and medical diagnosis and therapy require the magnetic particles to be stable in water at neutral pH and physiological salinity. The colloidal stability of this fluid will depend first, on the dimensions of the particles, which should be sufficiently small so that precipitation due to gravitation forces can be avoided, and second on the charge and surface chemistry, which give rise to both, steric and coulombic repulsions [26]. Additional restrictions to the possible particles that could be used for biomedical applications strongly depend on whether these particles are going to be used for *in vivo* or *in vitro* applications.

For *in vivo* applications the magnetic particles must be coated with a biocompatible polymer during or after the synthesis process to prevent the formation of large aggregates, changes from the original structure and biodegradation when exposed to the biological system. The polymer will also allow binding of drugs by covalent attachment, adsorption or entrapment on the particles [27, 28]. The important factors, which determine the biocompatibility and toxicity of these materials, are the nature of the magnetically responsive component, such as magnetite, iron, nickel, cobalt, neodymium–iron–boron or samarium–cobalt and the final size of the particles, their core and the coatings. Iron oxide particles such as magnetite (Fe_3O_4) or its oxidized form maghemite ($\gamma\text{-Fe}_2\text{O}_3$) are by far the most commonly employed for biomedical applications. Highly magnetic materials such as cobalt and nickel are toxic, susceptible to oxidation and hence are of little interest [21, 29]. Moreover, the main advantage of using particles of sizes smaller than 100 nm (so-called nanoparticles) is their higher effective surface areas (easier attachment of ligands), lower sedimentation rates (high stability) and improved tissular diffusion [30]. Another advantage of using nanoparticles is that the magnetic dipole–dipole interactions are significantly reduced because they scale as r^6 (r is the particle radius) [31–33]. Therefore, for *in vivo* biomedical applications, magnetic nanoparticles must be made of a non-toxic and non-immunogenic material, with particle sizes small enough to remain in the circulation after injection and to pass through the capillary systems of organs and tissues avoiding vessel embolism. They must also have a high magnetization so that their movement in the blood can be controlled with a magnetic field and so that they can be immobilized close to the targeted pathologic tissue [34].

For *in vitro* applications the size restrictions are not so severe as in *in vivo* applications. Therefore, composites

consisting of superparamagnetic nanocrystals dispersed in submicron diamagnetic particles with long sedimentation times in the absence of a magnetic field can be used. The advantage of using diamagnetic matrixes is that the superparamagnetic composites can be easily provided with functionality.

In almost all applications the preparation method of the nanomaterials represents one of the most important challenges that will determine the particle size and shape, the size distribution, the surface chemistry of the particles and consequently their magnetic properties. Ferri- and ferromagnetic materials such as Fe_3O_4 , $\text{SrFe}_{12}\text{O}_{19}$, Fe–C and some alloys like SmCo_5 , have irregular particle shape when obtained by grinding bulk materials but can have a spherical shape when prepared by wet chemistry, plasma atomization or from the aerosol and gas phases. Also, depending on the mechanism of formation, spherical particles obtained in solution can be amorphous or crystalline if they result from a disordered or ordered aggregation of crystallites, respectively. In addition, the preparation method determines to a great extent the degree of structural defects or impurities in the particle, as well as the distribution of such defects within the particle and therefore its magnetic behaviour [16, 35].

Recently many attempts have been made to develop processes and techniques that would yield ‘monodispersed colloids’ consisting of uniform nanoparticles both in size and shape [36–39]. In these systems, the entire uniform physicochemical properties directly reflect the properties of each constituent particle. Monodispersed colloids have been exploited in fundamental research and as models in the quantitative assessment of properties that depend on the particle size and shape. In addition, it has become evident that the quality and reproducibility of commercial products can be more readily achieved by starting with well-defined powders of known properties. In this way, these powders have found application in photography, inks in high-speed printing, ceramic, catalysis, and especially in medicine.

The first part of this review deals with the possible use of magnetic nanoparticles for biomedical application with special emphasis on the advantage of using nanoparticles with respect to microparticles. The second part is concerned with different methods described in the bibliography capable of producing these magnetic nanoparticles with very narrow particle size distribution, mainly based on magnetite or maghemite iron oxide nanoparticles [21, 29]. Finally, we address some of the most relevant synthesis effects on the structural and magnetic properties of the magnetic nanoparticles.

2. Biomedical applications

We can classify biomedical applications of magnetic nanoparticles according to their application inside (*in vivo*) or outside (*in vitro*) the body. *In vivo* applications could be further separated in therapeutic (hyperthermia and drug-targeting) and diagnostic applications (nuclear magnetic resonance (NMR) imaging), while for *in vitro* applications the main use is in diagnostic (separation/selection, and magnetorelaxometry).

2.1. *In vivo* applications

2.1.1. Therapeutic applications

Hyperthermia. Hyperthermia is a therapeutic procedure used to raise the temperature of a region of the body affected by malignancy or other growths. It is administered together with other cancer treatments (multimodal oncological strategies). The rationale is based on a direct cell-killing effect at temperatures above 41–42°C [40–43]. Modern clinical hyperthermia trials focus mainly on the optimization of thermal homogeneity at moderate temperatures (42–43°C) in the target volume. The temperature increase required for hyperthermia can be achieved, among other methods, by using fine iron oxide magnetic particles [44]. The physical principle for which a magnetic material can be heated by the action of an external alternating magnetic field are the loss processes that occur during the reorientation of the magnetization of magnetic materials with low electrical conductivity [45, 46].

The advantage of magnetic hyperthermia is that allows the heating to be restricted to the tumour area. Moreover, the use of subdomain magnetic particles (nanometre-sized) is preferred instead multidomain (micron-sized) particles because nanoparticles absorb much more power at tolerable AC magnetic fields [42, 47–49]. Finally, it should be mentioned that the heating potential is strongly dependent on the particle size and shape, and thus having well-defined synthetic routes able to produce uniform particles is essential for a rigorous control in temperature.

Drug delivery. Since the pioneering concept proposed by Freeman *et al* [50] that fine iron particles could be transported through the vascular system and be concentrated at a particular point in the body with the aid of a magnetic field (figure 1), the use of magnetic particles for the delivery of drugs or antibodies to the organs or tissues altered by diseases has become an attractive field of research [51, 52].

The process of drug localization using magnetic delivery systems is based on the competition between forces exerted on the particles by blood compartment, and magnetic forces generated from the magnet, i.e. applied field. When the magnetic forces exceed the linear blood flow rates in arteries (10 cm s⁻¹) or capillaries (0.05 cm s⁻¹), the magnetic particles

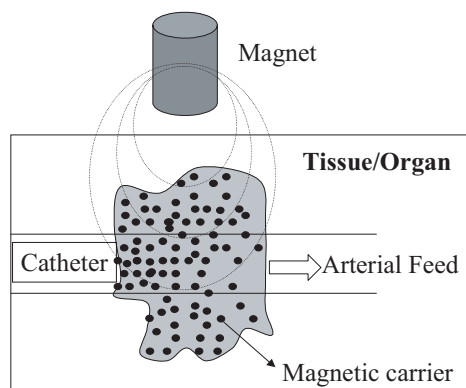


Figure 1. Schematic representation of the magnetically driven transport of drugs to a specific region. A catheter is inserted into an arterial feed to the tumour and a magnetic stand is positioned over the targeted site.

are retained at the target site and maybe internalized by the endothelial cells of the target tissue [51]. For this application the use of nanoparticles favour the transport through the capillary systems of organs and tissues avoiding vessel embolism.

2.1.2. Diagnostic applications

NMR imaging. The development of the NMR imaging technique for clinical diagnosis has prompted the need for a new class of pharmaceuticals, so-called magneto-pharmaceuticals. These drugs must be administered to a patient in order to (1) enhance the image contrast between normal and diseased tissue and/or (2) indicate the status of organ functions or blood flow [53]. A number of different agents have been suggested as potential NMR contrast agents. Most contrast agents used in NMR imaging studies to date have been paramagnetic. Superparamagnetic particles represent an alternative class of NMR contrast agents that are usually referred to as T_2 (transversal relaxation time) or T_2^* contrast agents as opposed to T_1 (longitudinal relaxation time) agents such as paramagnetic Gadolinium(III) chelates [21].

The relaxation rate increase produced by magnetic particles is a contribution of several complex mechanisms. The particles possess very large magnetic moments in the presence of a static magnetic field, and dipolar interactions between the superparamagnetic cores and surrounding solvent protons result in an increase in both longitudinal and transverse relaxation rates, especially for particles with diameters below 10 nm [54–56].

Commercial iron oxide nanoparticles of maghemite (Endorem® and Resovit®) have been used as contrast agents in NMR imaging for location and diagnosis of brain and cardiac infarcts, liver lesions or tumours, where the magnetic nanoparticles tend to accumulate at higher levels due to the differences in tissue composition and/or endocytotic uptake processes [57]. Especially promising results have been detected in the improvement of sensitivity of detection and delineation of pathological structures, such as primary and metastatic brain tumours, inflammation and ischemia [58]. For this purpose, proteins such as transferrin [59], peptides such as the membrane traslocating tat peptide of the HIV tat protein [60, 61], and oligonucleotides of various sequences [62] have been attached to aminated cross-linked iron oxide nanoparticles in order to obtain specific NMR imaging agents [63].

2.2. *In vitro* applications

2.2.1. Diagnostic applications

Separation and selection. At present, considerable attention is being paid to solid-phase extraction (SPE) as a way to isolate and preconcentrate desired components from a sample matrix. SPE offers an excellent alternative to the conventional sample concentration methods, such as liquid–liquid extraction [64]. The separation and preconcentration of the substance from large volumes of solution can be highly time consuming when using standard column SPE, and is in this field where the use of magnetic or magnetizable adsorbents called magnetic solid-phase extraction (MSPE) gains importance. In this procedure the magnetic adsorbent is added to a solution or suspension containing the target. This is adsorbed onto the

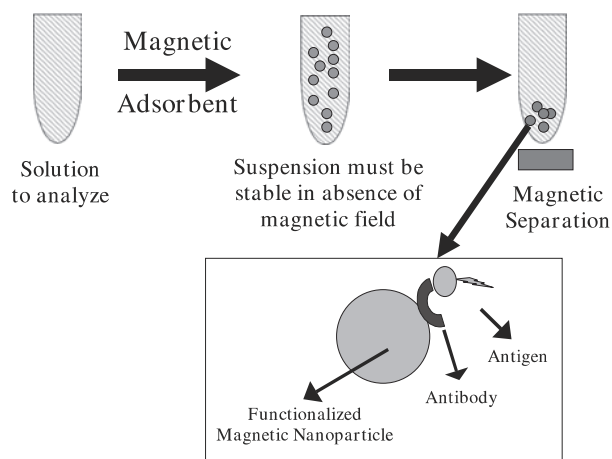


Figure 2. Schematic representation of the magnetically assisted separation of substances. In this particular case a magnetic nanosphere to which an antibody has been anchored is dispersed in a liquid medium containing the antigen (substance to analyse).

magnetic adsorbent and then the adsorbent with the adsorbed target is recovered from the suspension using an appropriate magnetic separator (figure 2). For separation and selection the advantage of using magnetic nanoparticles instead magnetic microparticles is that we can prepare suspensions that are stable against sedimentation in absence of an applied magnetic field. The applicability of iron oxide magnetic nanoparticles in MSPE is clearly evidenced by the fact that already exists in the market companies (DYNAL Biotech) that commercialize these products.

Magnetorelaxometry. Recently, magnetorelaxometry was introduced as a method for the evaluation of immunoassays [65]. Magnetorelaxometry measures the magnetic viscosity, i.e. the relaxation of the net magnetic moment of a system of magnetic nanoparticles after removal of a magnetic field [66].

There are two different relaxation mechanisms. First, the internal magnetization vector of a nanoparticle relaxes in the direction of the easy axis inside the core; this is called Néel relaxation [67]. Second, particles accomplish rotational diffusion in a carrier liquid, called Brownian relaxation [66]. Néel and Brownian relaxation can be distinguished by their different relaxation times [68]. Furthermore, Brownian relaxation can take place only in liquids, whereas Néel relaxation does not depend on the dispersion of the nanoparticles. The fact that magnetorelaxometry depends on the core size, the hydrodynamic size and the anisotropy allows this technique to distinguish between free and bound conjugates by their different magnetic behaviour, and therefore can be used as an analytical tool for the evaluation of immunoassays [66]. For this application the benefits of reducing particle size to the nanometre-sized are similar to those described for separation and selection applications.

2.3. Future applications

Magnetically directed microspheres containing radionuclides have been used for internal radiotherapy [51]. However, little work has been done in the use of magnetic nanoparticles in radiotherapy. One strategy under active investigation to

improve dose localization is that of administration of drugs, metabolites, etc that have been labelled with radioactive isotopes in a quantity sufficient to deactivate the tumour cells [69]. In this way, the use of surface-activated magnetic nanoparticles could have tremendous impact in improving the efficiency of the cancer treatments.

We can even envisage a future in which magnetic particles could be used for the repair of the human body with prosthetics or artificial replacement parts. In this field special mention deserves the pioneering work of Dailey *et al* [70] who have reported the synthesis of a silicone based magnetic fluid for use in eye surgery. Retinal detachment is a major cause of vision loss in adults. It occurs when the retina separates from the choroid, resulting in eventual death of the retina and subsequent loss of vision. Dailey and co-workers have developed an internal tamponade from modified silicone fluid containing sterically stabilized 4–10 nm sized metal particles, which will be held in place with an external magnetized scleral buckle.

3. Synthesis methods

One of the latest tendencies in materials science is to tailor-make classical products with controlled properties for special uses. Particular attention should be paid to the preparation methods that allow the synthesis of particles nearly of uniform size and shape. This goal can be achieved by precipitation from a homogeneous solution under controlled conditions or by controlling the particle growth in a process where a precursor in aerosol or vapour form is decomposed. Examples of such preparations include gold colloids, sulfur sols, metal oxides and hydrous oxides [36–38, 71, 72].

In the case of magnetic nanoparticles for biomedical applications we have classified the synthesis methods into those that produce magnetic nanoparticles from solution techniques or from aerosol/vapour phases, and those producing composites consisting of magnetic nanoparticles dispersed in submicron-sized organic or inorganic matrixes that usually have spherical shape. Finally, we have also described briefly another group of methods that use size selection principles to produce uniform nanoparticles starting from polydisperse particles.

3.1. Magnetic nanoparticles

3.1.1. Precipitation from solution. In general these methods allow the preparation of magnetic nanoparticles with a rigorous control in size and shape in a simple rather way and thus are very appropriate for their use in biomedical applications. Uniform particles are usually prepared via homogeneous precipitation reactions, a process that involves the separation of the nucleation and growth of the nuclei [38]. A schematic representation of the different mechanisms proposed in the bibliography to explain the formation of uniform particles is shown in figure 3.

In a homogeneous precipitation, a short single burst of nucleation occurs when the concentration of constituent species reaches critical supersaturation. Then, the nuclei so obtained are allowed to grow uniformly by diffusion of solutes from the solution to their surface until the final size is

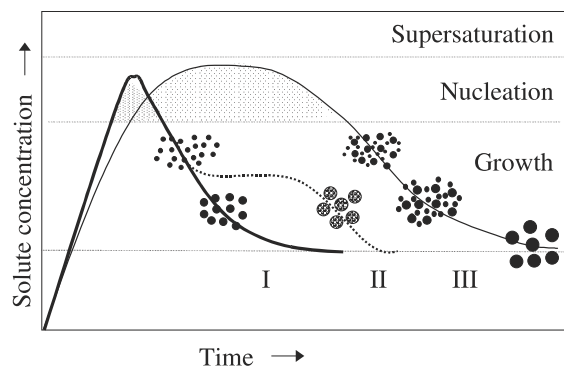


Figure 3. Mechanism of formation of uniform particles in solution: curve I: single nucleation and uniform growth by diffusion (classical model of LaMer and Dinegar); curve II: nucleation, growth and aggregation of smaller subunits; curve III: multiple nucleation events and Ostwald ripening growth.

attained. To achieve monodispersity, these two stages must be separated and nucleation should be avoided during the period of growth. This is the classical model proposed by LaMer and Dinegar [73] first to explain the mechanism of formation of sulfur colloids and also for a limited number of cases (curve I of figure 3). However, uniform particles have also been obtained after multiple nucleation events. The uniformity of the final product is in this case achieved through a self-sharpening growth process (Ostwald ripening, curve III of figure 3) [74]. In addition, uniform particles have also been obtained as a result of aggregation of much smaller subunits rather than continuous growth by diffusion (curve II of figure 3) [75–77]. An artificial separation between nucleation and growth processes may be achieved by seeding in which foreign particles are introduced into the solution of monomers below the critical supersaturation [38].

The most important methods described in the bibliography to obtain uniform iron-based nanoparticles in solution are briefly described in the following sections: coprecipitation, microemulsions, the polyol process and decomposition of organic precursors.

Coprecipitation. There are two main methods for the synthesis in solution of magnetite spherical particles in the nanometre range. In the first, ferrous hydroxide suspensions are partially oxidized with different oxidizing agents [77]. For example, spherical magnetite particles of narrow size distribution with mean diameters between 30 and 100 nm can be obtained from a Fe(II) salt, a base and a mild oxidant (nitrate ions) [77].

The other method consists in ageing stoichiometric mixtures of ferrous and ferric hydroxides in aqueous media, yielding spherical magnetite particles homogeneous in size [78]. In addition, it has been shown that by adjusting the pH and the ionic strength of the precipitation medium, it is possible to control the mean size of the particles over one order of magnitude (from 15 to 2 nm) [79]. The size decreases as the pH and the ionic strength in the medium increases [79]. Both parameters affect the chemical composition of the surface and consequently, the electrostatic surface charge of the particles. Under these conditions, magnetite particles are formed by aggregation of primary particles formed within an $\text{Fe}(\text{OH})_2$ gel. This is an ordered aggregation that gives rise to spherical

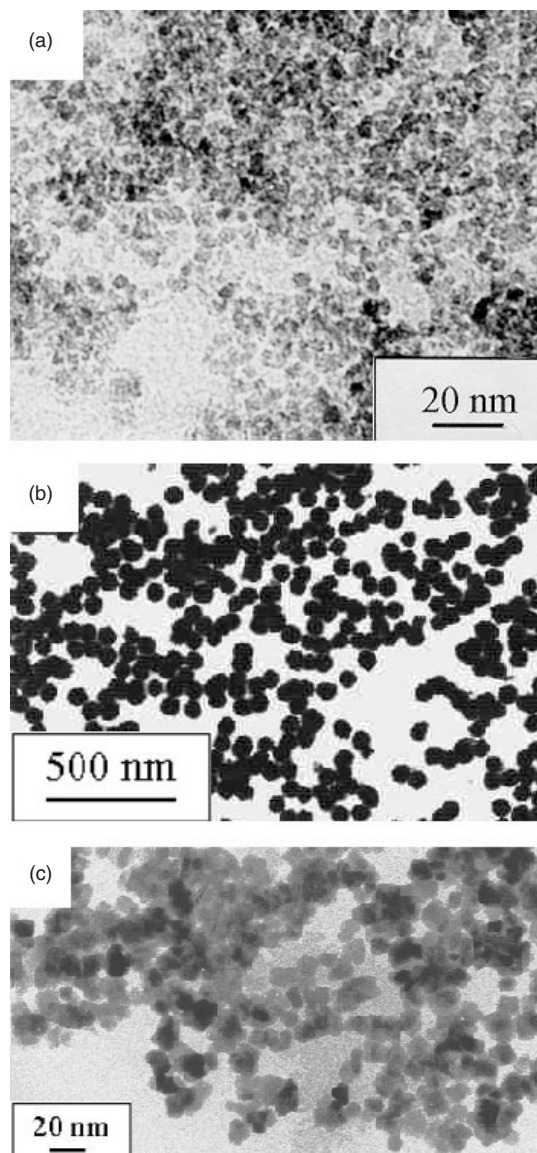


Figure 4. Magnetic nanoparticles prepared in solution by: (a) coprecipitation (maghemite). (b) Polyol process (Fe-based alloy). Reprinted from [38]. (c) Microemulsions (maghemite). Reprinted from [91].

crystalline particles [77]. The smallest particles can also be generated after adding polyvinylalcohol (PVA) to the iron salts [80]. A typical microstructure of magnetic nanoparticles produced by this method is shown in figure 4.

Modifications of this method allow for synthesis in the presence of dextran or any other substance that renders the magnetic nanoparticles biocompatible and thus make this method especially appropriate for *in vivo* applications [81, 82]. In fact, this is the most common method used to obtain the commercial NMR contrast agents based on magnetic nanoparticles. For example, nanosized magnetic particles are obtained by transferring an acidic iron(II)/iron(III) salt solution into iron(II,III)-carbonate by adding equivalent amounts of alkaline carbonate, followed by thermal oxidation. [83] The size of the particles can be controlled by the thermal reaction velocity and concentration of the iron salts. Thus, small diameters in the range of 20–100 nm can be obtained by

timely separation of iron(II,III)-carbonate at temperatures of 5–10°C and subsequent heating. After surplus salts have been removed, the particles can be stabilized with water-soluble polysaccharide- or synthetic polymer derivatives. Nanoparticles coated with a starch derivative have a molar mass of 10 kDa. As a result of the starch matrix, the magnetic particles can retain their dispersion stability in the pH range 3–12 and also in high salt concentrations [173].

Microemulsions. Water-in-oil (W/O) microemulsions (i.e. reverse micelle solutions) are transparent, isotropic, thermodynamically stable liquid media. In these systems, fine microdroplets of the aqueous phase are trapped within assemblies of surfactant molecules dispersed in a continuous oil phase. The surfactant-stabilized microcavities (typically in the range of 10 nm) provide a confinement effect that limits particle nucleation, growth, and agglomeration [84]. W/O microemulsions have been shown to be an adequate, versatile, and simple method to prepare nanosized particles [85–90] and these are the characteristics that could make this method useful for both *in vivo* and *in vitro* applications.

Pileni and co-workers [91] prepared nanosized magnetic particles with average sizes from 4 to 12 nm and standard deviation ranging from 0.2 to 0.3 using microemulsions. A ferrous dodecyl sulfate, $\text{Fe}(\text{DS})_2$, micellar solution was used to produce nanosized magnetic particles whose size is controlled by the surfactant concentration and by temperature. A typical microstructure of magnetic nanoparticles produced by this method is shown in figure 4. Magnetite nanoparticles around 4 nm in diameter have been prepared by the controlled hydrolysis with ammonium hydroxide of FeCl_2 and FeCl_3 aqueous solutions within the reverse micelle nanocavities generated by using AOT as surfactant and heptane as the continuous oil phase [92].

Carpenter and co-workers [93] prepared metallic iron particles coated by a thin layer of gold via a microemulsion. The gold shell protects the iron core against oxidation and also provides functionality, making these composites applicable in biomedicine. The reverse micelle reaction is carried out using cetyltrimethylammonium bromide (CTAB) as the surfactant, octane as the oil phase, and aqueous reactants as the water phase [94]. The metal particles are formed inside the reverse micelle by the reduction of a metal salt using sodium borohydride. The sequential synthesis offered by reverse micelles is utilized to first prepare an iron core by the reduction of ferrous sulfate by sodium borohydride. After the reaction has been allowed to go to completion, the micelles within the reaction mixture are expanded to accommodate the shell using a larger micelle containing additional sodium borohydride. The shell is formed using an aqueous hydrogen tetrachloroaurate solution.

Polyols. A very promising technique for the preparation of uniform nanoparticles that could be used in biomedical applications such as magnetic resonance imaging is the polyol technique. Fine metallic particles can be obtained by reduction of dissolved metallic salts and direct metal precipitation from a solution containing a polyol [36, 38]. This process was first used to prepare noble metals such as Ru, Pd, Pt, Au, and others such as Co, Ni or Cu [95, 96]. Latterly, the process

has been extended to the synthesis of other materials such as Fe-based alloys [97, 98], which could be used for biomedical applications.

In the polyol process, the liquid polyol acts as the solvent of the metallic precursor, the reducing agent and in some cases as a complexing agent for the metallic cations. The metal precursor can be highly or only slightly soluble in the polyol. The solution is stirred and heated to a given temperature reaching the boiling point of the polyol for less reducible metals. By controlling the kinetic of the precipitation, non-agglomerated metal particles with well-defined shape and size can be obtained. A better control of the average size of the metal particles can be obtained by seeding the reactive medium with foreign particles (heterogeneous nucleation). In this way, nucleation and growth steps can be completely separated and uniform particles result.

Iron particles around 100 nm can be obtained by disproportionation of ferrous hydroxide in organic media [99]. $\text{Fe}(\text{II})$ chloride and sodium hydroxide reacts with ethylene glycol (EG) or polyethylene glycol (PEG) and the precipitation occurs in a temperature range as low as 80–100°C. Furthermore, iron alloys can be obtained by coprecipitation of Fe, Ni, and/or Co in EG and PEG. Monodispersed quasi-spherical and non-agglomerated metallic particles with mean size around 100 nm have been obtained without seeding (homogeneous nucleation) while particles between 50 and 100 nm have been obtained using Pt as the nucleating agent (heterogeneous nucleation). Whereas FeCo particles are formed by agglomerates of Fe and Co primary particles produced over different lengths of time, spherical FeNi particles present good homogeneity as a result of concomitant Fe and Ni formation and growth by the aggregation of nm-sized primary particles [98]. A typical microstructure of magnetic nanoparticles produced by the polyol process is shown in figure 4.

High-temperature decomposition of organic precursors. The decomposition of iron precursors in the presence of hot organic surfactants has yielded markedly improved samples with good size control, narrow size distribution and good crystallinity of individual and dispersible magnetic iron oxide nanoparticles. Biomedical applications like magnetic resonance imaging, magnetic cell separation or magnetorelaxometry strongly depend on particle size and thus magnetic nanoparticles produced by this method could be potentially used for these applications.

For example, Alivisatos and co-workers [100] have demonstrated that injecting solutions of FeCup_3 (Cup: *N*-nitrosophenylhydroxylamine) in octylamine into long-chain amines at 250–300°C yields nanocrystals of maghemite. These nanocrystals range from 4 to 10 nm in diameter, are crystalline, and are dispersible in organic solvents (figure 5). Hyeon and co-workers [101] have also been able to prepare monodisperse maghemite nanoparticles by a non-hydrolytic synthetic method. For example, to prepare maghemite nanoparticles of 13 nm (figure 5), $\text{Fe}(\text{CO})_5$ was injected into a solution containing surfactants and a mild oxidant (trimethylamine oxide).

Very recently, Sun and Zeng [102] have been able to prepare monodispersed magnetite nanoparticles with sizes

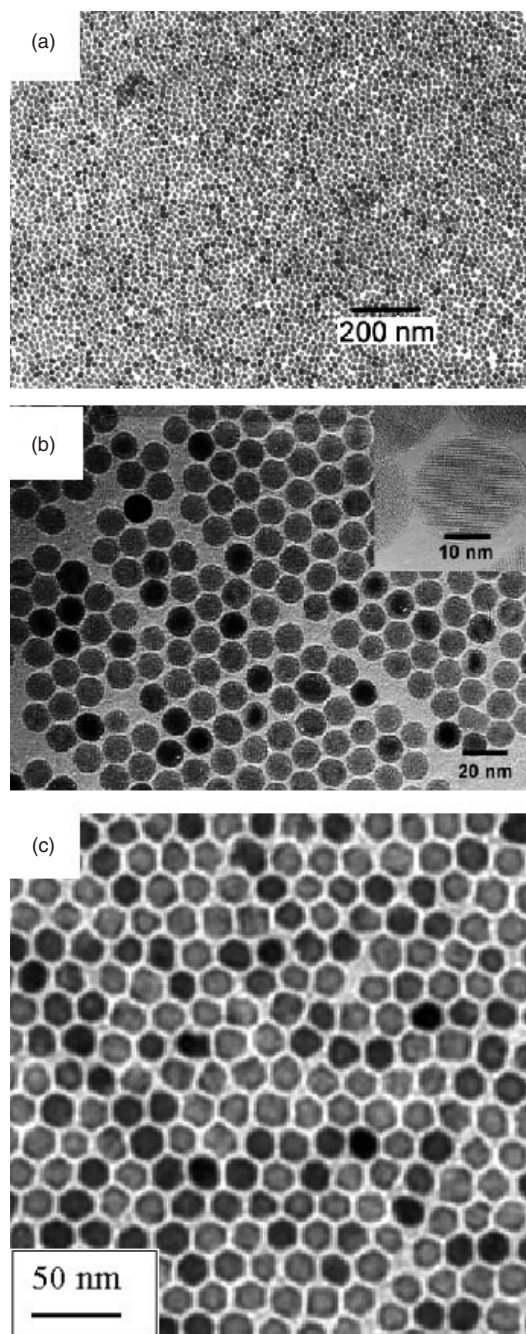


Figure 5. Maghemite nanoparticles prepared in solution by decomposition at high temperature of organic precursors: (a) FeCup_3 . Reprinted from [100]. (b) $\text{Fe}(\text{CO})_5$. Reprinted from [101]. (c) $\text{Fe}(\text{III})$ acetylacetonate. Reprinted from [102].

from 3 to 20 nm by the high-temperature (265°C) reaction of iron(III) acetylacetonate in phenyl ether in the presence of alcohol, oleic acid, and oleylamine (figure 5). In particular, magnetite nanoparticles around 4 nm were obtained by the thermal decomposition of the iron precursor but to obtain diameters up to 20 nm a seed-mediated growth method was required.

Other solution techniques. Here we describe a series of methods for the production of magnetic nanoparticles that could be mainly used for *in vivo* applications. Nature has

developed a variety of protein components that function as carriers or storage devices for metal components. Of these systems, the iron-storage protein ferritin is probably the most intensively studied and best understood [103]. Ferritin consists of a central core of hydrated iron(III) oxide encapsulated with a multisubunit protein shell. As a result of the inner diameter of the nanoreactors, Mann and co-workers have been able to prepare magnetite [104] and magnetite/maghemite nanoparticles [105] of about 6–7 nm in diameter. The magnetite/maghemite particles were generated by oxidation of apoferritin (empty ferritin) with trimethylamino-*N*-oxide, which was loaded with various amounts of iron(II) ions.

Of special interest is the use of dendrimers as templating hosts for the production of magnetic nanoparticles. In particular, by the judicious selection of the dendrimers it could be possible to prepare in a single-step biocompatible magnetic nanoparticles that could be used for *in vivo* applications. Recently, iron ferrite nanoparticles have been prepared using dendrimers as templating hosts [106]. Carboxylated poly(amidoamine) PAMAM dendrimers (generation 4.5) were utilized for the synthesis and stabilization of ferrimagnetic iron oxide nanoparticles. Oxidation of Fe(II) at slightly elevated pH and temperature resulted in the formation of highly soluble nanocomposites of iron oxides and dendrimer, which are stable under a wide range of temperatures and pHs.

Sonochemical-assisted synthesis has also been reported as an adequate method for the production of magnetite and maghemite nanoparticles [107–109]. In sonochemistry, the acoustic cavitation, that is, the formation, growth, and implosive collapse of a bubble in an irradiated liquid, generates a transient localized hot spot, with an effective temperature of 5000 K and a nanosecond lifetime [110]. The cavitation is a quenching process, and hence the composition of the particles formed is identical to the composition of the vapour in the bubbles, without phase separation.

Electrochemical methods have also been used for the production of maghemite nanoparticles [111]. The electrochemical synthesis of nanoparticles of $\gamma\text{-Fe}_2\text{O}_3$ was performed in an organic medium. The size was directly controlled by the imposed current density, and the resulting particles were stabilized as a colloidal suspension by the use of cationic surfactants. The size distributions of the particles were narrow, with the average sizes varying from 3 to 8 nm.

3.1.2. Aerosol/vapour methods. Spray and laser pyrolysis have been shown to be excellent techniques for the direct and continuous production of well-defined magnetic nanoparticles under exhaustive control of the experimental conditions. Their high-production rate can anticipate a promising future for the preparation of magnetic nanoparticles useful in *in vivo* and *in vitro* applications. The main difference between spray and laser pyrolysis is the final state of the ultrafine particles. In spray pyrolysis, the ultrafine particles are usually aggregated into larger particles, while in laser pyrolysis the ultrafine particles are less aggregated due to the shorter reaction time.

Spray pyrolysis. Spray pyrolysis is a process in which a solid is obtained by spraying a solution into a series of reactors where the aerosol droplets undergo evaporation of the solvent and solute condensation within the droplet, followed by drying and

thermolysis of the precipitated particle at higher temperature [112]. This procedure gives rise to microporous solids, which finally sinter to form dense particles.

This method represents a convenient procedure for obtaining finely dispersed particles of predictable shape, size, and variable composition. The resulting powders generally consist of spherical particles, the final diameter of which can be predetermined from that of the original droplets. The method offers certain advantages over other more commonly used techniques (such as precipitation from homogenous solution) as it is simple, rapid, and continuous. Recently, for example has been used for the production of materials with relevant properties, say mesoporous microspheres [113] and phosphorescent nanoparticles [114].

Most of the pyrolysis based processes employed to produce maghemite nanoparticles start with a Fe^{3+} salt and some organic compound that acts as the reducing agent. It was shown that in this procedure Fe^{3+} is partially reduced to a mixture of Fe^{2+} and Fe^{3+} in the presence of organic compounds with the formation of magnetite, which is finally oxidized to maghemite. Without the presence of a reducing agent, hematite is formed instead of maghemite [115].

In alcoholic solutions, uniform $\gamma\text{-Fe}_2\text{O}_3$ particles can be prepared with a wide variety of particle morphologies and sizes, ranging from 5 to 60 nm, depending on the nature of the iron precursor salt [116]. A detailed description of the device used for the preparation of these particles can be found in reference [117] and a schematic representation is given in figure 6. The device essentially consists in an aerosol droplet generator (atomizer, ultrasonic, etc), a furnace and a particle recovery system. Dense aggregates with spherical shape composed of $\gamma\text{-Fe}_2\text{O}_3$ subunits with a mean diameter of 6 and 60 nm have been obtained using Fe(III) nitrate and Fe(III) chloride solutions, respectively. On the other hand, $\gamma\text{-Fe}_2\text{O}_3$ obtained from acetylacetonate solutions resulted in monodispersed particles of about 5 nm in diameter while maghemite particles derived from Fe(II) ammonium citrate appeared as hollow spheres with a mean diameter of 300 nm. The latter consisted of small crystallites aggregated forming a shell, the size of which varied between 10 and 40 nm, depending on the heating temperature in the furnace. A typical microstructure of magnetic nanoparticles produced by this method is shown in figure 7.

Laser pyrolysis. Since the pioneering work of Cannon and co-workers [118] on the continuous production of nanometric powders by laser-induced processes, different powders such

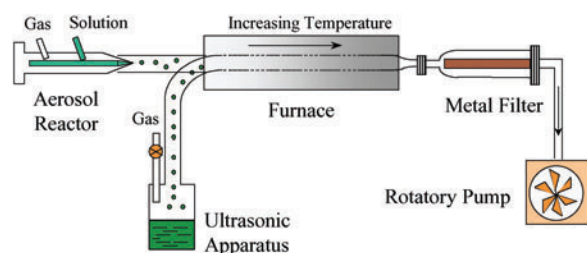


Figure 6. Schematic representation of the spray pyrolysis device used for the preparation of maghemite nanoparticles. This device consists of an aerosol generator (atomizer or an ultrasonic bath), one furnace and a particle recovery system.

as Si, SiC, Si_3N_4 and a Si/C/N composite have been prepared under a variety of conditions with sizes ranging from 5 to 20 nm [118, 119]. The method involves heating a flowing mixture of gases with a continuous wave carbon dioxide laser, which initiates and sustains a chemical reaction. Above a certain pressure and laser power, a critical concentration of nuclei is reached in the reaction zone, which leads to homogeneous nucleation of particles that are further transported to a filter by an inert gas. Three characteristics of this method must be emphasized: (a) the small particle size, (b) the narrow particle size distribution, and (c) the nearly absence of aggregation.

Pure, well-crystallized and uniform $\gamma\text{-Fe}_2\text{O}_3$ nanoparticles can be obtained in one single step by a CO_2 laser pyrolysis method (figure 7). Samples with particles of 3.5 and 5 nm in size and very narrow size distribution have been obtained under different experimental conditions [120, 121]. A schematic representation of the CO_2 laser pyrolysis device used for the preparation of the magnetic nanocrystals is shown in figure 8. In the device shown in figure 8, a small reaction zone is defined by the overlap between the vertical reactant gas stream and the horizontal laser beam. The reaction zone is safely separated from the chamber walls. This design provides an ideal environment for the nucleation of small particles in the nanometre range, with less contamination and narrower size distribution than those prepared by more conventional thermal methods.

To obtain the $\gamma\text{-Fe}_2\text{O}_3$ nanoparticles $\text{Fe}(\text{CO})_5$ (iron pentacarbonyl) was used as precursor. Due to the fact that this precursor does not absorb the radiation at the laser wavelength

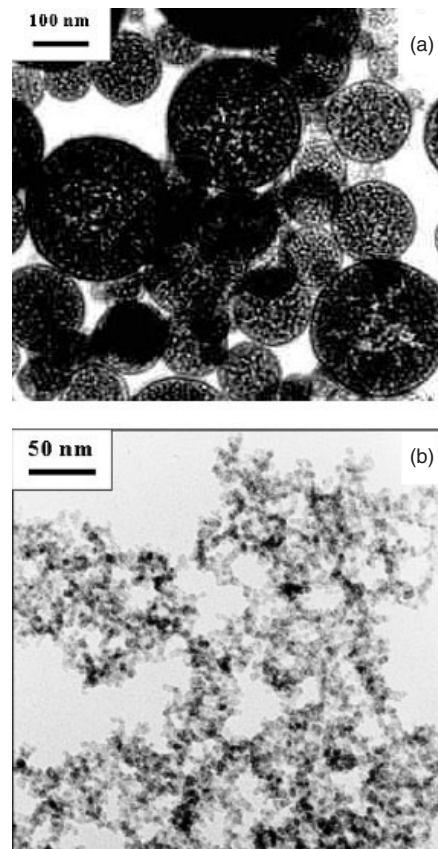


Figure 7. Magnetic nanoparticles of maghemite prepared by: (a) Spray pyrolysis. (b) Laser pyrolysis. Reprinted from [35].

($10.60 \pm 0.05 \mu\text{m}$), ethylene was used as absorbent as well as the carrier to transport the carbonyl vapour to the reaction zone. Ethylene does not decompose at the energy density used (652 W cm^{-2}) but simply absorbs the laser radiation heating the iron pentacarbonyl, which is decomposed into iron and carbon monoxide. In order to obtain iron oxide, air has to be introduced into the system, either with the iron pentacarbonyl vapour causing oxidation under the laser radiation or mixed with argon.

3.2. Magnetic composites

For separation processes i.e. *in vitro* applications we can use composites consisting of superparamagnetic nanocrystals dispersed in submicron diamagnetic matrixes that have long sedimentation times in the absence of a magnetic field. An advantage of using diamagnetic matrixes is that the superparamagnetic composite can be easily provided with functionality and biocompatibility. We now describe some of the most promising methods for the production of superparamagnetic composites that could be useful in the field of separation.

3.2.1. Deposition methods. Inorganic and hybrid coatings (or shells) on colloidal templates have been prepared by precipitation and surface reactions [122–126]. By the adequate selection of the experimental conditions, mainly the nature of the precursors, temperature, and pH, this method can give uniform, smooth coatings, and therefore lead to monodispersed spherical composites. Using this technique submicrometre-sized anionic polystyrene (PS) lattices have been coated with

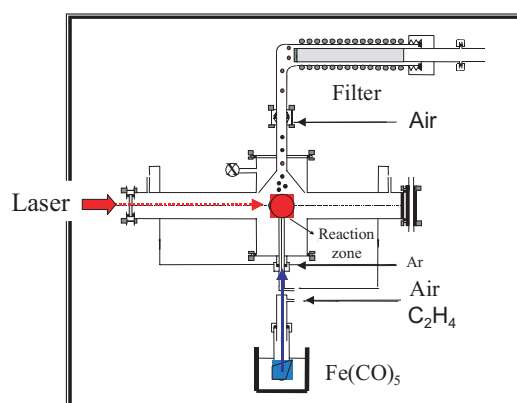


Figure 8. Schematic representation of the Laser pyrolysis device used for the preparation of maghemite nanoparticles around 5 nm in size.

uniform layers of iron compounds [127, 128] by ageing, at elevated temperature, dispersions of the polymer colloid in the presence of aqueous solutions of ferric chloride, urea, hydrochloric acid, and polyvinylpyrrolidone.

One of the most promising techniques for the production of superparamagnetic composites is the layer-by-layer (LBL) self-assembly method. This method was firstly developed for the construction of ultrathin films [129, 130] and further developed by Caruso *et al* [131, 132] for the controlled synthesis of novel nanocomposites core-shell materials and hollow capsules. It consists in the stepwise adsorption of charged polymers or nanocolloids and oppositely charged polyelectrolytes onto flat surfaces or colloidal templates, exploiting primarily electrostatic interactions for layer buildup (figure 9).

Using this strategy, colloidal particles have been coated with alternating layers of polyelectrolytes, nanoparticles, and proteins [132]. Furthermore, Caruso *et al* have demonstrated that submicrometre-sized hollow silica spheres [131] or polymer capsules [133] can be obtained after removal of the template from the solid-core multilayered-shell particles either by calcination or by chemical extraction. Special mention deserves their work in the preparation of iron oxide superparamagnetic and monodisperse dense and hollow spherical particles [134, 135] that could be used for biomedical applications (figure 10).

3.2.2. Encapsulation of magnetic nanoparticles in polymeric matrixes. Encapsulation of inorganic particles into organic polymers endows particles with important properties that bare uncoated particles lack [136]. Polymer coatings on particles enhance compatibility with organic ingredients, reduce susceptibility to leaching, and protect particle surfaces from oxidation. Consequently, encapsulation improves dispersibility, chemical stability, and reduces toxicity [137].

Polymer-coated magnetite nanoparticles have been synthesized by seed precipitation polymerization of methacrylic acid and hydroxyethyl methacrylate in the presence of the magnetite nanoparticles [138]. Cross-linking of polymers has also been reported an adequate method for the encapsulation of magnetic nanoparticles. To prepare the composites by this method, first, mechanical energy needs to be supplied to create a dispersion of magnetite in the presence of aqueous albumin [139], chitosan [140], or PVA polymers [141]. More energy creates an emulsion of the magnetic particle sol in cottonseed [139], mineral [140], or vegetable oil [141]. Depending upon composition and reaction conditions the addition of a cross-linker and heat results in polydispersed magnetic

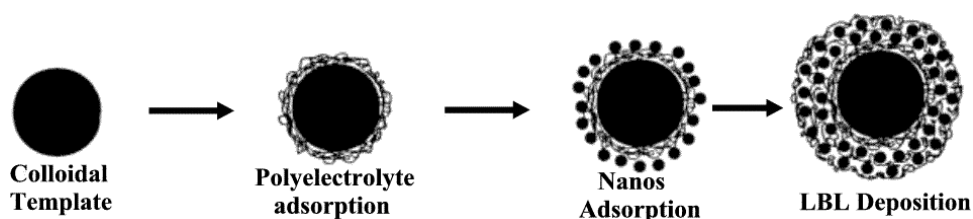


Figure 9. Schematic illustration of the LBL electrostatic assembly of nanoparticles onto spherical colloidal templates. Nanoparticles are adsorbed onto the polyelectrolyte because they have opposite charge density.

latex, 0.3 microns in diameter, with up to 24 wt% in magnetite content [139].

Recently, the preparation of superparamagnetic latex via inverse emulsion polymerization has been reported [29]. A 'double-hydrophilic' diblock copolymer, present during the precipitation of magnetic iron oxide, directs nucleation, controls growth, and sterically stabilizes the resulting 5 nm superparamagnetic iron oxide. After drying, the coated particles reprecipitate creating a ferrofluid-like dispersion. Inverse emulsification of the ferrofluid into decane, aided by small amounts of diblock copolymer emulsifier along with ultrasonication, creates minidroplets (180 nm) filled with magnetic particles and monomer. Subsequent polymerization generates magnetic latex.

A novel approach to prepare superparamagnetic polymeric nanoparticles by synthesis of the magnetite core and polymeric shell in a single inverse microemulsion was reported by Chu and co-workers [142]. Stable magnetic nanoparticle dispersions with narrow size distribution were thus produced. The microemulsion seed copolymerization of methacrylic acid, hydroxyethyl methacrylate, and cross-linker resulted in a stable hydrophilic polymeric shell around the nanoparticles. Changing the monomer concentration and water/surfactant ratio controls the particle size.

3.2.3. Encapsulation of magnetic nanoparticles in inorganic matrixes. An appropriate tuning of the magnetic properties is essential for the potential use of the superparamagnetic composites. In this way, the use of inorganic matrixes, in particular of silica, as dispersion media of superparamagnetic nanocrystals has been reported to be an

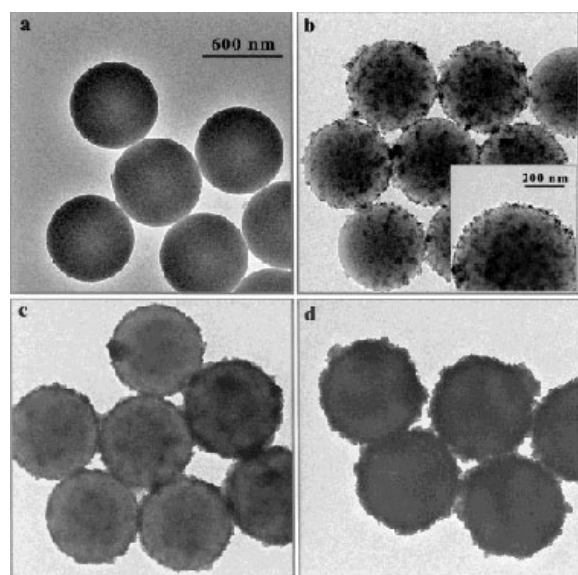


Figure 10. TEM micrographs of uncoated PS particles (a) and PS particles pre-coated with a three layer polyelectrolyte film and [Fe₃O₄/PAH] (b), [Fe₃O₄/PAH]₄ (c), and [Fe₃O₄/PDADMAC]₄ (d). PAH is a cationic polyelectrolyte (poly(allylamine hydrochloride)) and PDADMAC is also a cationic polyelectrolyte (poly(diallyldimethylammonium chloride)). The deposited Fe₃O₄ nanoparticles can be seen existing as aggregates. The magnetite loading on the particles increases with additional depositions of Fe₃O₄ and polycation. The scale bar corresponds to all four TEM images shown. Reprinted from [134].

effective way to modulate the magnetic properties by a simple heating process [143–145].

Another advantage of having a surface enriched in silica is the presence of surface silanol groups that can easily react with alcohols and silane coupling agents [146] to produce dispersions that are not only stable in non-aqueous solvents but also provide the ideal anchorage for covalent bounding of specific ligands. The strong binding makes desorption of these ligands a difficult task. In addition, the silica surface confers high stability to suspensions of the particles at high volume fractions, changes in pH or electrolyte concentration [147].

Recently, we have been successful in preparing submicronic silica coated maghemite hollow and dense spheres with a high loading of magnetic material by aerosol pyrolysis [148, 149]. Silica coated γ -Fe₂O₃ hollow spherical particles with an average size of 150 nm (figure 11) were prepared by the aerosol pyrolysis of methanol solutions containing iron ammonium citrate and tetraethoxysilane (TEOS) at a total salt concentration of 0.25 M [148]. An illustration of the possible formation mechanism of the silica coated magnetic hollow spheres is shown in figure 11. During the first stage the rapid evaporation of the methanol solvent favours the surface precipitation (i.e. formation of hollow spheres) of components [112]. The low solubility of the iron ammonium citrate in methanol when compared with that of TEOS promotes the initial precipitation of the iron salt solid shell. During the second stage the probable continuous shrinkage of this iron salt solid shell facilitates the enrichment at the surface of the silicon oxide precursor (TEOS). In the third stage, the thermal decomposition of precursors produces the silica coated γ -Fe₂O₃ hollow spheres. The formation of the γ -Fe₂O₃ is associated with the presence of carbonaceous species coming from the decomposition of the methanol solvent and from the iron ammonium citrate and TEOS. On the other hand, the aerosol pyrolysis of iron nitrate and TEOS at a total salt concentration of 1 M produced silica coated γ -Fe₂O₃ dense

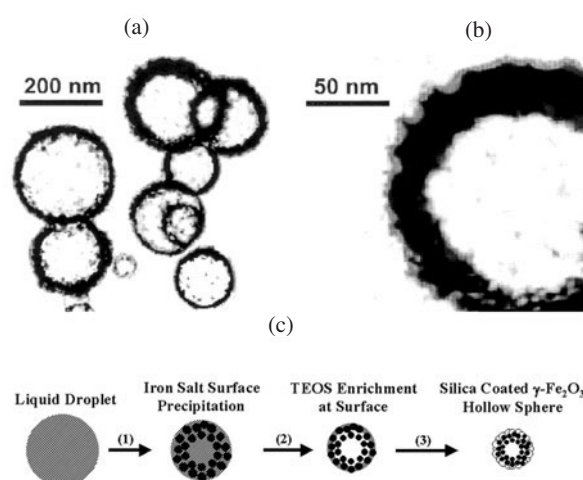


Figure 11. (a) TEM picture of the silica/iron oxide composites prepared by aerosol pyrolysis of a mixture of iron ammonium citrate and TEOS. (b) Details of a hollow spherical particle showing an outer particle layer mainly constituted (according to TEM microanalyses) by SiO₂. (c) Illustration of the formation mechanism of the silica coated γ -Fe₂O₃ hollow particles. Reprinted from [148].

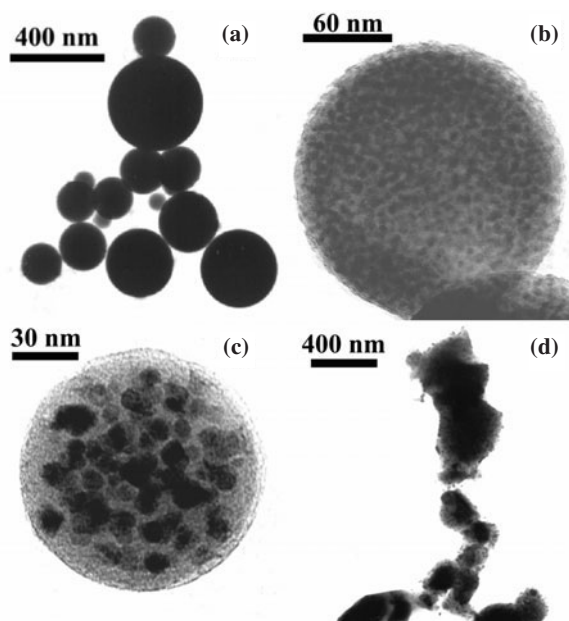


Figure 12. TEM micrographs of the silica/iron oxide composites prepared by aerosol pyrolysis of a mixture of iron nitrate (20 mol%) and TEOS (a) and further heated in a conventional furnace for 2 h at 900°C (b), 1050°C (c), and 1200°C (d). Note in the sample heated at 1050°C the presence of γ -Fe₂O₃ (dark regions) nanoparticles smaller than 20 nm dispersed in a microspherical silica particle (lighter regions). At this temperature, the enrichment of silica on particle outerlayers is clearly observed. It is important to note that similar microstructures to that shown in micrographs (b) and (c) were observed for smaller and bigger particles. Note also the high stability of the spherical magnetic composites (the particles lost spherical shape only temperatures of 1200°C as a consequence of a sintering process). Reprinted from [149].

spherical particles with an average size of 250 nm (figure 12). The increase in salt concentration to a value of 1 M favours the formation of dense spherical particles. Sedimentation studies of these particles have shown that are particularly useful for separation applications [149].

A W/O microemulsion method has also been used for the preparation of silica-coated iron oxide nanoparticles [150]. Three different non-ionic surfactants (Triton X-100, Igepal CO-520, and Brij-97) have been used for the preparation of microemulsions, and their effects on the particle size, crystallinity, and the magnetic properties have been studied. The iron oxide nanoparticles are formed by the coprecipitation reaction of ferrous and ferric salts with inorganic bases. A strong base, NaOH, and a comparatively mild base, NH₄OH, have been used with each surfactant to observe whether the basicity influences the crystallization process during particle formation. All these systems show magnetic behaviour close to that of superparamagnetic materials. By use of this method, magnetic nanoparticles as small as 1–2 nm and of very uniform size (standard deviation less than 10%) have been synthesized. A uniform silica coating as thin as 1 nm encapsulating the bare nanoparticles is formed by the base-catalysed hydrolysis and the polymerization reaction of TEOS in the microemulsion. It is worth mentioning that the small particle size of the composite renders these particles a potential candidate for their use in *in vivo* applications.

3.3. Size selection methods

Biomedical applications like magnetic resonance imaging, magnetic cell separation or magnetorelaxometry utilize the magnetic properties of the nanoparticles in magnetic fluids. Furthermore, these applications also depend on the hydrodynamic size. Therefore, in many cases only a small portion of particles contributes to the desired effect. The relative amount of the particles with the desired properties can be increased by the fractionation of magnetic fluids [66, 151].

Common methods currently used for the fractionation of magnetic fluids are centrifugation [152] and size-exclusion chromatography [153]. All these methods separate the particles via non-magnetic properties like density or size. Massart *et al* [154] have proposed a size sorting procedure based on the thermodynamic properties of aqueous dispersions of nanoparticles. The positive charge of the maghemite surface allows its dispersion in aqueous acidic solutions and the production of dispersions stabilized through electrostatic repulsions. By increasing the acid concentration (in the range 0.1–0.5 mol l⁻¹), interparticle repulsions are screened and phase transitions are induced. Using this principle, these authors describe a two-step size sorting process, in order to obtain significant amounts of nanometric monosized particles with diameters between typically 6 and 13 nm. As the surface of the latter is not modified by the size sorting process, usual procedures are used to disperse them in several aqueous or oil-based media.

Preference should be given, however, to partitions based on the properties of interest, in this case the magnetic properties. So far, magnetic methods have been used only for the separation of magnetic fluids, for example, to remove aggregates by magnetic filtration [155]. Recently, the fractionation of magnetic nanoparticles by flow field–flow fractionation was reported [156]. Field–flow fractionation is a family of analytical separation techniques [157], in which the separation is carried out in a flow with a parabolic profile running through a thin channel. An external field is applied at a right angle to force the particles toward the so-called accumulation wall [151].

4. Effect of synthesis on the magnetic properties

4.1. Particle size and structural effects

We now present some of our results that clearly manifest the importance of controlling the particle size and the structure to produce magnetic materials with a defined magnetic response for a specific biomedical application. It should be taken into account that size and structural effects are parameters that can be controlled through the synthesis methods. On the other hand, magnetite and maghemite are by far the most used materials for biomedical application and therefore this study is focused on these materials.

Magnetite has a cubic inverse spinel structure with oxygen forming a fcc close packing and Fe cations occupying interstitial tetrahedral sites and octahedral sites [158]. Maghemite has a structure similar to that of magnetite, only differs in that all or most of the Fe is in the trivalent state (figure 13). Cation vacancies compensate for the oxidation of Fe(II) cations [158]. Maghemite has a cubic unit cell in

which each cell contains 32 O ions, $21\frac{1}{3}$ iron(III) ions and $2\frac{1}{3}$ vacancies. The cations are distributed over the 8 tetrahedral and 16 octahedral sites, whereas the vacancies are confined to the octahedral sites. Synthetic maghemite often displays superstructure forms, which arises as a result of the cations and the vacancy ordering. The extent of vacancy ordering is related to both the crystallite size and the amount of iron(II) in the structure or other impurities [159]. All of these possible arrangements in the maghemite are partially responsible for the different magnetic behaviour manifested by maghemite nanoparticles prepared by different synthetic routes [35].

The extent of vacancy ordering inside γ -Fe₂O₃ nanoparticles can be easily observed by registering the infrared spectra of different maghemite samples [35] (figure 14). Thus, in the samples prepared by solution techniques (coprecipitation), the one with the largest particle size (14 nm) shows the infrared features of γ -Fe₂O₃ crystallites, which are at least partially ordered, as evidenced by the multiple lattice absorption bands between 800 and 200 cm⁻¹. Meanwhile, in the sample with the lowest particle size (5 nm) a significant reduction in the number of lattice absorption bands associated with increasing disorder is detected [160]. Note the difference

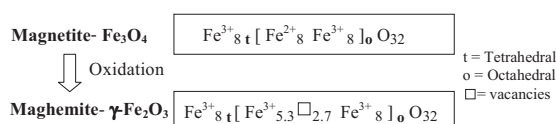


Figure 13. Chemical formula for the magnetite/maghemite system. The order of the vacancies in the octahedral positions of the maghemite can lead to a tetragonal superstructure (unit-cell is three times the cubic one).

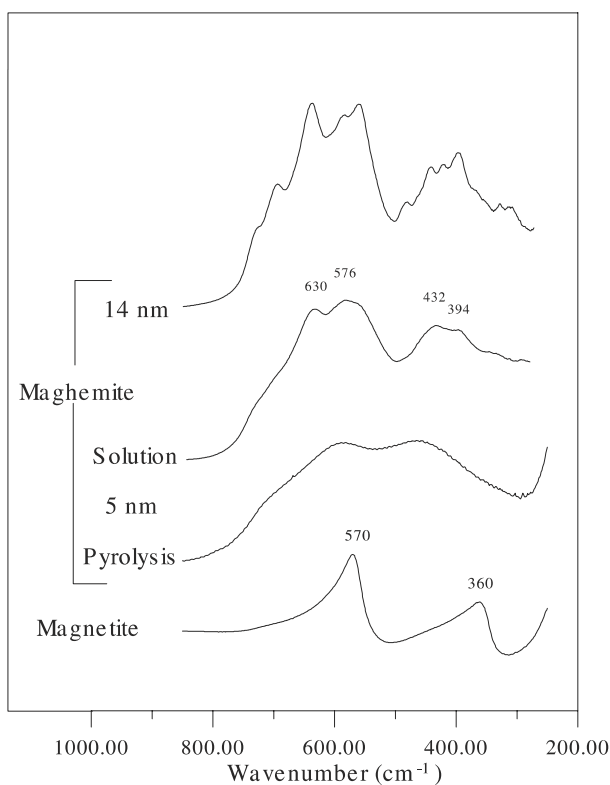


Figure 14. Infrared spectra for magnetite and maghemite nanoparticles prepared by different methods.

in the infrared spectra of two samples that have a similar particle size (5 nm) but have been prepared by two different techniques (solution and pyrolysis). Particularly, the infrared spectrum of the sample prepared by pyrolysis only displays two broad maximum at around 600 and 450 cm⁻¹ indicating a random distribution of vacancies and therefore is expected to behave differently in the presence of an applied magnetic field. We also note from figure 14 that infrared spectroscopy is a simple tool to differentiate between maghemite and magnetite crystalline phases.

It has been shown that the degree of order in the distribution of cation vacancies, inherent in the γ -Fe₂O₃ structure, of particles smaller than ~ 100 nm affects the magnetic properties, suggesting that magnetic moments in the interior of the particles can be significantly influenced by canting effects [161]. For nanometre γ -Fe₂O₃ particles, this effect could explain at least in part the reduction in saturation magnetization found at very small sizes. In fact, the existence of magnetically disordered layers around the particles have been proposed by various researchers as the particle size approaches the frontier of 10 nm [162, 163]. The proposed effects are in many cases, however, obscured by a wide distribution of particle sizes and shapes or by magnetic interactions between particles. The effect of the size and structural ordering on the magnetic properties of γ -Fe₂O₃ nanoparticles (<20 nm) has been carried out in uniform samples prepared by coprecipitation from solution and laser pyrolysis methods [35]. The results are shown in figure 15. A progressive cation disorder that strongly affects the saturation magnetization values is found in γ -Fe₂O₃ nanoparticles as the particle size decreases. The smallest particles, where some vacancy order is observed, are of about 8 nm in diameter. In general, when the particles are obtained by pyrolysis, the saturation magnetization is smaller than for samples prepared by precipitation from solution.

Direct information about the directions of the atomic moments in nanoparticles can be obtained by Mössbauer spectroscopy. The Mössbauer spectra registered at 5 K in a magnetic field of 4 T applied parallel to the γ -radiation of uniform nanoparticles smaller than 5 nm prepared by laser pyrolysis (samples Laser1 and Laser2) and precipitation in

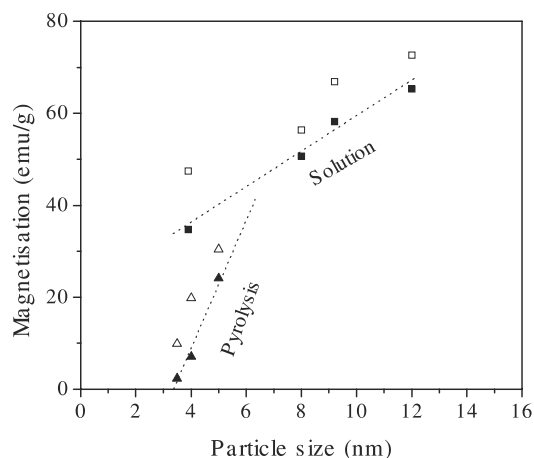


Figure 15. Saturation magnetization values of maghemite nanoparticles as a function of particle size and the preparation method (filled symbols: 298 K, empty symbols: 5 K).

solution (solution), are shown in figure 16 [164]. The fitting of the spectra of samples Laser1 and Laser2 results in a non-zero relative area of lines 2 and 5, which are very slightly reduced by the applied field. The main effect was in the line broadening which affects the lines 1 and 6, suggesting that the directions of the atomic moments are highly disordered for the laser samples due to a high degree of canting and spin frustration. In contrast, the spectrum of a maghemite sample of similar particle size (between 3 and 5 nm), prepared by precipitation in the presence of oleic acid shows well resolved A and B sites and can be fitted with two sextets. The area of lines 2 and 5 correspond to average canting angles of about 20° and 33° , much smaller than the canting observed with samples Laser1 and Laser2. The effect of the preparation method on the magnetic disorder is clearly demonstrated by the spectra shown in figure 16 for sample Laser1, and especially for sample Laser2. The fit of these spectra gives average hyperfine fields slightly smaller than those of conventional microcrystalline maghemite particles (about 52 T), and the hyperfine fields decrease with the particle crystallinity to about 48 T for sample Laser2. This decrease in the average hyperfine fields is presumably also due to the increase in the internal magnetic disorder [164].

4.2. Interaction effects

The wide variety of magnetic behaviour of nanostructured materials is complicated by interparticle interactions, which limits their possible application in biomedicine. For

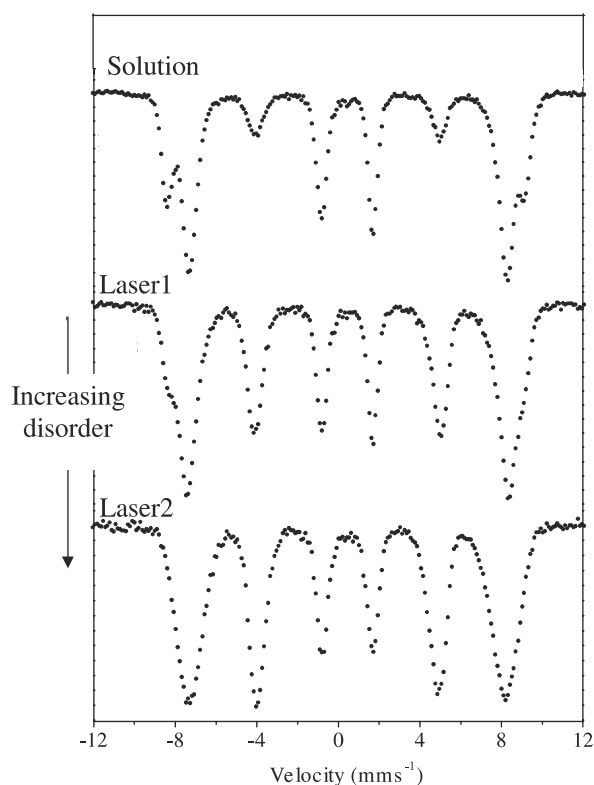


Figure 16. Mössbauer spectra at 5 K in the presence of a magnetic field of 4 T applied parallel to the γ -radiation for maghemite nanoparticles prepared by different methods and with different degree of cationic disorder.

sufficiently dilute dispersions, interparticle interactions usually of a dipolar nature are negligible and the crossover to the blocked state with decreasing temperature depends only on the physical properties of the individual particles. However, at higher densities (usually needed in practical applications) interparticle interactions strongly affect the behaviour of the dispersion. In particular, dipolar interactions between particles cause frustration of the moments, which no longer align themselves precisely with the particles' easy axes at low T . Rather, as the dispersion is cooled, collective, glassy behaviour results. While this phenomenon has been studied extensively, most work to date has focused on shifts of the blocking temperature, and the subtle question of whether the cooperative freezing can be described as a true thermodynamic spin glass transition [165, 166].

We have examined the effect of interaction on the magnetic properties of composites in maghemite nanoparticles encapsulated in spherical silica particles that could be used for biomedical applications [149, 167]. In particular, we have analysed the results using zero field cooling (ZFC) experiments and the standard relation for the temperature variation of the reduced remanence (ratio between the remanence magnetization and the saturation magnetization extrapolated at 0 K, $M_r(0)/M_s(0)$) [168]. In the ZFC experiments we observed an increase of the temperature at which the ZFC peak reaches its cusp with the increase in volume packing fraction, which was associated with the increase in the interparticle interactions. On the other hand, the fact that $M_r(0)/M_s(0)$ values were in all cases below 0.5 was explained from the effect of competition between interparticle interactions and intraparticle anisotropy on the spin relaxation process, which produces frustration [168–170].

5. Final remarks

The search for new synthetic routes or the improvement of established ones which are able to produce reliable magnetic nanoparticles with the correct characteristics of improved tissular diffusion, colloidal stability and biocompatibility is in continuous development. If we can gain sufficient understanding and control of the biological reactions with the magnetic nanoparticle, we may be able to control the rejection of nanomagnets by the human body. Ultimately, new materials and understanding of their interaction with the body may lead to better biocompatible nanomagnets.

For example the application of magnetic liposomes (lipid vesicles, containing submicron-sized magnetic nanoparticles in their structure either in the lipid bilayer or in the aqueous compartment) as 'vehicles' for targeted drug delivery appears to be a promising technique [171]. Liposomes can be used for encapsulation of many biologically active substances, and can prolong their therapeutic action by gradual release of the drug. Magnetic components of the liposomes allow concentration of the liposomes in the desired area of the patient's organs by magnetic forces, often augmented by magnetic agglomeration. In this regard the work of Bulte and co-workers [172] is worthy of note. These authors have developed magnetic liposomes derivatized with the hydrophilic polymer polyethylene glycol (PEG) that may escape rapid uptake by cells of the endothelial system.

Drug and gene delivery will continue to impact significantly on the practice of biomedicine. Magnetic drug-targeting will undoubtedly dramatically improve the therapeutic potential of many water-insoluble and unstable drugs. The development of drugs able to target selected cells or organs within the body will also deeply improve the benefits of some of the *in vivo* biomedical applications of nanomagnets. In this field the work of Bergemann and co-workers [173] is worthy of note. These authors have succeeded in developing novel iron oxide magnetic nanoparticles to which ion-exchange groups were attached, thereby enabling simple and reversible binding of ligands. The remarkable feature of ionically bound pharmaceutical drugs to the surface of particulate drug delivery systems is that the active low molecular weight substances can desorb from the carriers after a defined time span and hence diffuse from the vascular wall into the tissue.

Acknowledgments

The authors would like to thank K O'Grady for proof reading the manuscript. This research was supported by CICYT under projects MAT2000-1504 and MAT2002-04001-C02. The financial support from the regional government of Madrid under project CAM 07N/0057/2002 is also gratefully acknowledged. PT acknowledges the financial support from the Ramon y Cajal program.

References

- [1] Niemeyer C M 2001 *Angew. Chem. Int. Ed.* **40** 4128
- [2] Hood J D, Bednarski M, Frausto R, Guccione S, Reisfeld R A, Xiang R and Cheresh D A 2002 *Science* **296** 2404
- [3] Grainger D W and Okano T 2003 *Adv. Drug Del. Rev.* **55** 311
- [4] Whitesides G and Alivisatos A P 1999 Fundamental scientific issues for nanotechnology *Nanotechnology Research Directions* ed A P Alivisatos *et al* (IWGN Workshop Report)
- [5] El-Sayed M A 2001 *Acc. Chem. Res.* **34** 257
- [6] Heath J R 1995 *Science* **270** 1315
- [7] Murray C B, Kagan R and Bawendi M G 1995 *Science* **270** 1335
- [8] Zhang J Z 1997 *Acc. Chem. Res.* **30** 423
- [9] Bohren C F and Huffman D R 1983 *Absorption and Scattering of Light by Small Particles* (New York: Wiley)
- [10] Kung H and Foeke T 1999 *MRS Bull.* **24** 14
- [11] Hahn H, Logas J and Averbach R S 1990 *J. Mater. Reson.* **5** 609
- [12] Zhou Y C and Rahaman M N 1993 *J. Mater. Reson.* **8** 1680
- [13] Tartaj P and Tartaj J 2002 *Acta Materialia* **50** 5
- [14] Tartaj J, Zarate J, Tartaj P and Lachowski E E 2002 *Adv. Eng. Mater.* **4** 17
- [15] Niihara K 1991 *J. Ceram. Soc. Japan* **99** 974
- [16] Battle X and Labarta A 2002 *J. Phys. D: Appl. Phys.* **35** R15
- [17] Frenkel J and Dorfman J 1930 *Nature* **126** 274
- [18] Bean C P and Livingston J D 1959 *J. Appl. Phys.* **30** 1205
- [19] Berkovsky B M, Medvedev V F and Krovov M S 1993 *Magnetic Fluids: Engineering Applications* (Oxford: Oxford University Press)
- [20] Charles S W and Popplewell J 1986 Properties and applications of magnetic liquids *Hand Book of Magnetic Materials* vol 2, ed K H J Buschow, p 153
- [21] Merbach A E and Tóth E 2001 *The Chemistry of Contrast Agents in Medical Magnetic Resonance Imaging* (Chichester, UK: Wiley)
- [22] Hilbert I, Andra W, Bahrng R, Daum A, Hergt R and Kaiser W A 1997 *Invest. Radiol.* **32** 705
- [23] Bangs L B 1996 *Pure Appl. Chem.* **68** 1873
- [24] Joubert J C 1997 *Anales de Quimica Int Ed.* **93** S70
- [25] Rye P D 1996 *Bio/Technology* **14** 155
- [26] Langer R 1990 *Science* **249** 1527
- [27] Häfeli U, Schütt W, Teller J and Zborowski M 1997 *Scientific and Clinical Applications of Magnetic Carriers* (New York: Plenum)
- [28] Denizot B, Tanguy G, Hindre F, Rump E, Lejeune J J and Jallet P 1999 *J. Colloid Interface Sci.* **209** 66
- [29] Wormuth K 2001 *J. Colloid Interface Sci.* **241** 366
- [30] Portet D, Denizot B, Rump E, Lejeune J J and Jallet P 2001 *J. Colloid Interface Sci.* **238** 37
- [31] Philipse A P, van Bruggen M P and Pathmamanoharan C 1994 *Langmuir* **10** 92
- [32] Garcell L, Morales M P, Andres-Verges M, Tartaj P and Serna C J 1998 *J. Colloid Interface Sci.* **205** 470
- [33] Butter K, Bomans P H H, Frederik P M, Vroege G J and Philipse A 2003 *Nature Mater.* **2** 88
- [34] Jordan A, Scholz R, Maier-Hauff K, Johannsen M, Wust P, Nadobny J, Schirra H, Schmidt H, Deger S, Loening S, Lanksch W and Felix R 2001 *J. Magn. Magn. Mater.* **225** 118
- [35] Morales M P, Veintemillas-Verdaguer S, Montero M I, Serna C J, Roig A, Casas Ll, Martinez B and Sandiumenge F 1999 *Chem. Mater.* **11** 3058.
- [36] Matijevec E (ed) 1989 *Fine Particles* A special issue in MRS Bulletin **14** 18
- [37] Matijevec E 1993 *Chem. Mater.* **5** 412
- [38] Sugimoto T 2000 *Fine Particles: Synthesis, Characterisation and Mechanism of Growth* (New York: Marcel Dekker)
- [39] Younan X, Gates B, Yin Y and Lu Y 2000 *Adv. Mater.* **12** 693
- [40] Wust P, Hildebrandt B, Sreenivasa G, Rau B, Gellermann J, Riess H, Felix R and Schlag P M 2002 *Lancet Oncol.* **3** 487
- [41] Andrä W, d'Ambly C G, Hergt R, Hilger I and Kaiser A 1999 *J. Magn. Magn. Mater.* **194** 197
- [42] Jordan A, Scholz R, Wust P, Fählng H and Felix R 1999 *J. Magn. Magn. Mater.* **201** 413
- [43] Hilger I, Hergt R and Kaiser W A 2000 *Invest. Radiol.* **35** 170
- [44] Gilchrist R K, Medal R, Shorey W D, Hanselman R C, Parrott J C and Taylor C B 1957 *Ann. Surg.* **146** 596
- [45] Hiergeist R, Andrä W, Buske N, Hergt R, Hilger I, Richter U and Kaiser W 1999 *J. Magn. Magn. Mater.* **201** 420
- [46] Néel L 1949 *C.R. Acad. Sci.* **228** 664
- [47] Chan D C F, Kirpotin D B and Bunn P A 1993 *J. Magn. Magn. Mater.* **122** 374
- [48] Hilger I, Frühauf K, Andrä W, Hiergeist R, Hergt R and Kaiser W A 2002 *Acad. Radiol.* **9** 198
- [49] Rosensweig R E 2002 *J. Magn. Magn. Mater.* **252** 370
- [50] Freeman M W, Arrot A and Watson H H L 1960 *J. Appl. Phys.* **31** 404
- [51] Joubert J C 1997 *An. Quim. Int. Ed.* **93** S70
- [52] Goodwin S, Peterson C, Hoh C and Bittner C 1999 *J. Magn. Magn. Mater.* **194** 132
- [53] Coroiu I 1999 *J. Magn. Magn. Mater.* **201** 449
- [54] Ayant Y, Belorizky E, Alizon J and Gallice J 1975 *J. Phys. A* **36** 991
- [55] Freed J H 1978 *J. Chem. Phys.* **68** 4034
- [56] Morales M P, Bomati-Miguel O, Pérez de Alejo R, Ruiz-Cabello J, Veintemillas-Verdaguer S and O'Grady K 2003 *J. Magn. Magn. Mater.* at press
- [57] Kim D K, Zhang Y, Kher J, Klason T, Bjelke B and Muhammed M 2001 *J. Magn. Magn. Mater.* **225** 256
- [58] Roberts P L, Chuang N and Roberts H C 2000 *Eur. J. Rad.* **34** 166
- [59] Högemann D, Josephson L, Weissleder R and Basilion J P 2000 *Bioconjugate Chem.* **11** 941
- [60] Josephson L, Tung C H, Moore A and Weissleder R 1999 *Bioconjugate Chem.* **10** 186

- [61] Lewin M, Carlesso N, Tung C H, Tung X W, Cory D, Scadden D T and Weissleder R 2000 *Nat. Biotechnol.* **18** 410
- [62] Josephson L, Perez J M and Weissleder R 2001 *Angew. Chem. Int. Ed.* **40** 3204
- [63] Högemann D, Ntziachristos V, Josephson L and Weissleder R 2002 *Bioconjugate Chem.* **13** 116
- [64] Safarikova M and Safarik I 1999 *J. Magn. Magn. Mater.* **194** 108
- [65] Weitschies W, Köttitz R, Bunte T and Trahms L 1997 *Pharm. Pharmacol. Lett.* **7** 5
- [66] Rheinländer T, Köttitz R, Weitschies W and Semmler W 2000 *J. Magn. Magn. Mater.* **219** 219
- [67] Néel L 1949 *Ann. Geophys.* **5** 99
- [68] Köttitz R, Weitschies W, Trahms L, Brewer W and Semmler W 1999 *J. Magn. Magn. Mater.* **194** 62
- [69] Suit H 2002 *Int. J. Rad. Onc. Biol. Phys.* **53** 798
- [70] Dailey J P, Phillips J P, Li C and Riffle J S 1999 *J. Magn. Magn. Mater.* **194** 140
- [71] Matijevic E 1994 *Langmuir* **10** 8
- [72] Serna C J and Morales M P 2003 Maghemite (γ -Fe₂O₃): A versatile magnetic colloidal material *Surface and Colloid Science* Ch 2 ed E Matijevic and M Borkovec (New York: Kluwer/Plenum)
- [73] LaMer V K and Dinegar R H 1950 *J. Am. Chem. Soc.* **72** 4847
- [74] Den Ouden C J J and Thompson R W 1991 *J. Colloid Interface Sci.* **143** 77
- [75] Ocaña M, Rodriguez-Clemente R and Serna C J 1995 *Adv. Mater.* **7** 212
- [76] Morales M P, González-Carreño T and Serna C J 1992 *J. Mater. Reson.* **7** 2538
- [77] Sugimoto T and Matijevic E 1980 *J. Colloid Interface Sci.* **74** 227
- [78] Massart R and Cabuil V 1987 *J. Chem. Phys.* **84** 967
- [79] Jolivet J P 2000 *Metal Oxide Chemistry and Synthesis: From Solutions to Solid State* (New York: Wiley)
- [80] Lee J, Isobe T and Senna M 1996 *J. Colloid Interface Sci.* **177** 490
- [81] Molday R S and Mackenze D 1982 *J. Immunol. Method* **52** 353
- [82] Palmacci S and Josephson L 1993 *US Patent* 5262176
- [83] Bergemann C 1996 *German Patent* DE 19624426 A1
- [84] Pileni M P 1993 *J. Phys. Chem.* **97** 6961
- [85] Lisiecki I and Pileni M P 1993 *J. Am. Chem. Soc.* **7** 115
- [86] Zhang K, Chew C H, Xu G Q, Wang J and Gan L M 1999 *Langmuir* **15** 3056
- [87] Zarur A J and Ying J Y 2000 *Nature* **403** 65
- [88] Tartaj P and De Jonghe L C 2000 *J. Mater. Chem.* **10** 2786
- [89] Tartaj P and Tartaj J 2002 *Chem. Mater.* **14** 536
- [90] Pileni M P 2003 *Nature Mater.* **2** 145
- [91] Feltin N and Pileni M P 1997 *Langmuir* **13** 3927
- [92] López-Quintela M A and Rivas J 1993 *J. Colloid Interface Sci.* **158** 446
- [93] Carpenter E E 2001 *J. Magn. Magn. Mater.* **225** 17
- [94] Boutonnet M, Kizling J and Stenius P 1982 *Colloids Surf. A* **5** 209
- [95] Viau G, Ravel F, Acher O, Fievet-Vicent F and Fievet F 1994 *J. Appl. Phys.* **76** 6570
- [96] Fievet F, Lagier J P, Blin B, Beaudoin B and Figlarz M 1989 *Solid State Ionics* **32/33** 198
- [97] Viau G, Fievet-Vicent F and Fievet F 1996 *J. Mater. Chem.* **6** 1047
- [98] Viau G, Fievet-Vicent F and Fievet F 1996 *Solid State Ion.* **84** 259
- [99] Fievet F, Lagier J P, Blin B, Beaudoin B and Figlarz M 1989 *Solid State Ion.* **32/33** 198
- [100] Rockenberger J, Scher E C and Alivisatos A P 1999 *J. Am. Chem. Soc.* **121** 11595
- [101] Hyeon T, Lee S S, Park J, Chung Y and Na H B 2001 *J. Am. Chem. Soc.* **123** 12798
- [102] Shen S and Zeng H 2002 *J. Am. Chem. Soc.* **124** 8204
- [103] Chasteen N D and Harrison P M 1999 *J. Struct. Biol.* **126** 182
- [104] Meldrum F C, Heywood B R and Mann S 1992 *Science* **257** 522
- [105] Wong K K W, Douglas T, Gider S, Awschalom D D and Mann S 1998 *Chem. Mater.* **10** 279
- [106] Strable E, Bulte J W M, Moskowitz B, Vivekanandan K, Allen M and Douglas T 2001 *Chem. Mater.* **13** 2201
- [107] Cao X, Koltypin Y, Katabi G, Prozorov R, Felner I and Gedanken A 1997 *J. Mater. Res.* **12** 402
- [108] Shafi K V P M, Ulman A, Yan X, Yang N-L, Estournés C, White H and Rafailovich M 2001 *Langmuir* **17** 5093
- [109] Shafi K V P M, Ulman A, Dyal A, Yan X, Yang N-L, Estournés C, Fournes L, Wattiaux A, White H and Rafailovich M 2002 *Chem. Mater.* **14** 1778
- [110] Suslick K S 1990 *Science* **247** 1439
- [111] Pascal C, Pascal J L, Favier F, Elidrissi-Moubtassim M L and Payen C 1999 *Chem. Mater.* **11** 141
- [112] Messing G L, Zhang S and Jayanthi G V 1993 *J. Am. Ceram. Soc.* **76** 2707
- [113] Lu Y, Fan H, Stump A, Ward T L, Rhiiker T and Brinker C J 1999 *Nature* **398** 223
- [114] Xia B, Lenggoro I W and Okuyama K 2001 *Adv. Mater.* **13** 1579
- [115] Pecharroman C, González-Carreño T and Iglesias J E 1995 *Phys. Chem. Min.* **22** 21
- [116] González-Carreño T, Morales M P, Gracia M and Serna C J 1993 *Mater. Lett.* **18** 151
- [117] González-Carreño T, Mifsud A, Serna C J and Palacios J M 1993 *Mater. Chem. Phys.* **27** 287
- [118] Cannon W R, Danforth S C, Flint J H, Haggerty J S and Marra R A 1982 *J. Am. Ceram. Soc.* **65** 324
- [119] Cauchetier M, Croix O, Herlin N and Luce M 1994 *J. Am. Ceram. Soc.* **77** 93
- [120] Veintemillas-Verdaguer S, Morales M P and Serna C J 1998 *Mater. Lett.* **35** 227
- [121] Veintemillas-Verdaguer S, Morales M P and Serna C J 2001 *Appl. Organomet. Chem.* **15** 1
- [122] Garg A and Matijević E 1988 *Langmuir* **4** 38
- [123] Aiken B and Matijević E 1988 *J. Colloid Interface Sci.* **126** 645
- [124] Aiken B, Hsu W P and Matijević E 1990 *J. Mater. Sci.* **25** 1886
- [125] Ocaña M, Hsu W P and Matijević E 1991 *Langmuir* **7** 2911
- [126] Varanda L C, Tartaj P, González-Carreño T, Morales M P, Muñoz T, O'Grady K, Jafelicci M and Serna C J 2002 *J. Appl. Phys.* **92** 2079
- [127] Shiho H, Manabe Y and Kawahashi N 2000 *J. Mater. Chem.* **10** 333
- [128] Shiho H and Kawahashi N 2000 *J. Colloid Interface Sci.* **241** 366
- [129] Fendler J H 1998 *Nanoparticles and Nanostructured Films: Preparation, Characterization and Application* (Weinheim: Wiley-VCH)
- [130] Ulman A 1991 *An Introduction to Ultrathin Organic Films: From Langmuir-Blodgett to Self-Assembly* (Boston: Academic)
- [131] Caruso F, Caruso R A and Möhwald H 1998 *Science* **282** 1111
- [132] Caruso F 2001 *Adv. Mater.* **13** 11
- [133] Donath E, Sukborukov G B, Caruso F, Davies S A and Möhwald H 1998 *Angew. Chem. Int. Ed.* **37** 2201
- [134] Caruso F, Susa A S, Giersig M and Möhwald H 1999 *Adv. Mater.* **11** 950
- [135] Caruso F, Spasova M, Susa A, Giersig M and Caruso R A 2001 *Chem. Mater.* **13** 109
- [136] Ziolo R F, Giannelis E P, Weinstein B A, O'Horo M P, Ganguly B N, Mehrotra V, Russell M W and Huffman D R 1992 *Science* **257** 219
- [137] Bourgeat-Lami E and Lang J J 1998 *J. Colloid Interface Sci.* **197** 293
- [138] Zaitsev V S, Filimonov D S, Presnyakov I A, Gambino R J and Chu B 1999 *J. Colloid Interface Sci.* **212** 49

- [139] Gupta P K, Hung T C, Lam F C and Perrier D G 1988 *Int. J. Pharmaceutics* **43** 167
- [140] Hassan E E, Parish R C and Gallo J M 1992 *Pharm. Res.* **9** 390
- [141] Müller-Schulte D and Brunner D 1995 *J. Chromatogr. A* **711** 53
- [142] Dresco P A, Zaitsev V S, Gambino R J and Chu B 1999 *Langmuir* **15** 1945
- [143] Del Monte F, Morales M P, Levy D, Fernandez A, Ocaña M, Roig A, Mollins E, O'Grady K and Serna C J 1997 *Langmuir* **13** 3627
- [144] Ennas G, Musinu A, Piccaluga G, Zadda D, Gatteschi D, Sangregorio C, Stanger J L, Concas G and Spano G 1998 *Chem. Mater.* **10** 495
- [145] Tartaj P and Serna C J 2002 *Chem. Mater.* **14** 4396
- [146] Ulman A 1996 *Chem. Rev.* **96** 1533
- [147] Mulvaney P, Liz-Marzán L M, Giersig M and Ung T 2000 *J. Mater. Chem.* **10** 1259
- [148] Tartaj P, González-Carreño T and Serna C J 2001 *Adv. Mater.* **13** 1620
- [149] Tartaj P, González-Carreño T and Serna C J 2002 *Langmuir* **18** 4556
- [150] Santra S, Tapeç R, Theodoropoulou N, Dobson J, Hebard A and Tan W 2001 *Langmuir* **17** 6000
- [151] Rheinländer T, Roessner D, Weitschies W and Semmler W 2000 *J. Magn. Magn. Mater.* **214** 269
- [152] Sjögren C E, Johansson C, Naevestad A, Sontum P C, Briley-Saebo K and Fahlvik A K 1997 *Magn. Res. Imag.* **15** 55
- [153] Nunes A C and Yu Z C 1987 *J. Magn. Magn. Mater.* **65** 265
- [154] Lefebure S, Dubois E, Cabuil V, Neveu S and Massart R 1998 *J. Mater. Reson.* **13** 2975
- [155] O'Grady K, Stewardson H R, Chantrell R W, Fletcher D, Unwin D and Parker M R 1986 *IEEE Trans. Magn. Magn.* **22** 1134
- [156] Williams S K R, Lee H and Turner M M 1999 *J. Magn. Magn. Mater.* **194** 248
- [157] Giddings J C 1993 *Science* **260** 1456
- [158] Cornell R M and Schwertmann U 1996 *The Iron Oxides. Structure, Properties, Reactions, Occurrence and Uses* (VCH: Weinheim)
- [159] Haneda K and Morrish A H 1977 *Solid State Commun.* **22** 779
- [160] Morales M P, Pecharrroman C, González-Carreño T and Serna C J 1994 *J. Solid State Chem.* **108** 158
- [161] Morales M P, Serna C J, Bødker F and Mørup S 1997 *J. Phys. Condens. Matter* **9** 5461
- [162] Iglesias O and Labarta A 2001 *Phys. Rev. B* **63**
- [163] Coey J M D 1971 *Phys. Rev. Lett.* **27** 1140
- [164] Serna C J, Morales M P, Bødker F and Mørup S 2001 *Solid State Commun.* **118** 437
- [165] Dormann J L, Fiorani D and Tronc E 1997 *Adv. Chem. Phys.* **98** 283
- [166] Fiorani D, Testa A M, Lucari F, D'Orazio F and Romero H 2002 *Physica B* **320** 122
- [167] Tartaj P, González-Carreño T and Serna C J 2003 *J. Phys. Chem. B* **107** 20
- [168] El-Hilo M, O'Grady K and Chantrell R W 1992 *J. Magn. Magn. Mater.* **114** 295
- [169] Held G A, Grinstein G, Doyle H, Sun S and Murray C B 2001 *Phys. Rev. B* **64** 012408
- [170] Mørup S, Bødker F, Hendriksen P V and Linderroth S 1995 *Phys. Rev. B* **52** 287
- [171] Kuznetsov A A, Filippov V I, Alyautdin R N, Torshina N L and Kuznetsov O A 2001 *J. Magn. Magn. Mater.* **225** 95
- [172] Bulte J W M, de Cuyper M, Despres D and Frank J A 1999 *J. Magn. Magn. Mater.* **194** 204
- [173] Bergemann C, Müller-Schulte D, Oster J, Brassard L and Lübke A S 1999 *J. Magn. Magn. Mater.* **194** 45